Monitoring, Prediction and Mitigation of Disasters by Satellite Remote Sensing (MPMD-2004 Symposium), pp. 123-130, Hyogo, Japan 2004.1

123

Damage Detection Method Based on Normal Fluctuation of Digital Numbers in Multi-Temporal Middle-Resolution Images

Masayuki Kohiyama[1], Miguel Estrada[1] and Fumio Yamazaki[2]

[1]*Institute of Industrial Science, University of Tokyo, 4-6-1 Komaba, Meguro-ku, Tokyo 153-8505, Japan*
[2]*Department of Urban Environment Systems, Faculty of Engineering, Chiba University, Yayoi-cho, Inage-ku, Chiba 263-8522, Japan*

ABSTRACT: A new damage or change detection method using middle-resolution satellite images is proposed, which employs the probability distribution model of the digital number (DN) fluctuation in a normal condition and its significance test.   The DN fluctuation model is formulated by considering imaging process of a satellite sensor and image registration process.   The result thematic map is created from the significance level to reject the null hypothesis that the pixel DN can be considered as a sample of the DN fluctuation model.   The method overcomes the threshold setting problem in conventional change detection methods.

1 INTRODUCTION

Although high-resolution satellite imagery gathers people's attention with its imaging capability, middle-resolution satellite imagery (e.g. Landsat-TM, Landsat-ETM+, SPOT-HRV, and EOS/ASTER), of which ground sampling interval is larger than 10m, should be utilized for damage detection.   This is because of the following reasons: 1) its wider swath can depict the perspective view of wide-ranging disaster areas, 2) its ample archive of previously acquired images can provide a pre-event image of almost any place after a disaster reliably, and 3) the cost of the image per area is considerably lower than that of high-resolution one.   In addition, it is the commonly accepted that all the available information should serve for disaster relief activities, and thus, we have to promote researches to devise damage detection methods using middle-resolution imagery as well as higher-resolution one.

This paper proposes a new damage (change) detection method by introducing probability model of digital number (DN) fluctuation in an image pixel and its significance test.   The method overcomes the uncertainty, arbitrariness and difficulty of threshold setting in conventional change detection methods.   This is the generalized method from the method originally provided by Kohiyama *et al.* (2003) based on nighttime images.

2 THRESHOLD SETTING PROBLEM IN DAMAGE (CHANGE) DETECTION

Determining a threshold value to discriminate damage and no damage, or change and no change is a difficult task.   Many researchers have proposed change detection procedures: comparison of land cover classifications, multi-date classification, image differencing/ratioing, index differencing (e.g. vegetation index, tasseled-cap indices), principal components analysis, and change vector analysis (Singh, 1989).   But, in the final stage of most techniques, change and no change may be judged by a simple thresholding as a '0-1' binary response:

$$change(x, y) = \begin{cases} 0 & (f(\mathbf{DN}) \le T) \\ 1 & (f(\mathbf{DN}) > T) \end{cases} \tag{1}$$

where x and y mean the target location on the ground, the vector $\mathbf{DN}$ means DNs of satellite images (can also mean multi-temporal data), and T is the threshold value supplied empirically or statistically by the analyst. Once you introduce threshold values, you can evaluate the change in categorical attributes of the target areas, e.g. from forest to urban, from no change to change, etc.   But, in case of damage detection, we often face the lack of reference data of damage areas and a threshold value derived from few reference data is unreliable; moreover, a threshold value may change from region to region, and country to country because urban structures have such variety that a certain threshold may not be valid for a different city any longer.

Morisette *et al.* (1999) propose to use generalized linear models (GLMs) in change detection and to generate a thematic map of 'probability of (category) change'.   Kohiyama *et al.* (2000) propose to use the significance level in a thematic map.   Probability expression can help us to avoid the uncertainty and arbitrariness of

threshold values and has the great advantage that people easily understand the credibility of the evaluation result. However, GLMs such as logit and probit model require sample reference data in the regression analysis, and deficiency of reference images of earthquake damage and the above-mentioned regional differences prohibit us to employ GLMs.   Thus, a new approach is necessary to address these problems.

3   DIGITAL NUMBER AS RANDOM VARIABLE

Our proposing method to detect damage is based on a principle that DN of a fixed point can be considered as a random variable, which changes and fluctuates even in normal, non-disaster situation.   This section explains how DN can be modeled into random variable based on the overall sensor model of electro-optical remote-sensing system (Schowengerdt, 1997).   In scanning operation of a satellite sensor, the radiance of band b, s_b is converted into the electric signal e_b:

$$e_b(x, y) = \iint s_b(\alpha, \beta) PSF(x - \alpha, y - \beta) \, d\alpha d\beta \qquad (2)$$

where PSF is the point spread function (PSF) of the whole sensor system, and this includes optical process.   As an example, the PSF of Landsat/TM is shown in Fig. 1(Schowengerdt, 1997).   The A/D converter samples and quantizes the electric signal into discrete DN values, $P(x, y)$:

$$P(x, y) = \text{int}(gain_b \times e_b(x, y) + offset_b) \qquad (3)$$

where $gain_b$ and $offset_b$ represents the parameters of the linear A/D conversion.

These equations include conversion from continuous to discrete spatial coordinates implicitly.   Usually, the discrete coordinates are different among images, and there exists a difference of the *sample-scene phase*, or pixel center offset, that is the relative location of the pixels and the target.   The relative spatial phase is unpredictable and mostly unknown for any given image acquisitions, and we assume it follows the two-dimensional uniform probability distribution between ± 1/2 pixel for both cross-track and in-track direction.

In analysis using multi-temporal images, all the images are registered and the offsets are adjust to the single reference image.   The cubic convolution is one of the most popular interpolation methods in this registration process:

$$Q(x, y) = \text{int}([\text{sinc}(1+t) \quad \text{sinc}(t) \quad \text{sinc}(1-t) \quad \text{sinc}(2-t)] \begin{bmatrix} P_{11} & P_{12} & P_{13} & P_{14} \\ P_{21} & P_{22} & P_{23} & P_{24} \\ P_{31} & P_{32} & P_{33} & P_{34} \\ P_{41} & P_{42} & P_{43} & P_{44} \end{bmatrix} \begin{bmatrix} \text{sinc}(1+s) \\ \text{sinc}(s) \\ \text{sinc}(1-s) \\ \text{sinc}(2-s) \end{bmatrix}) \qquad (4)$$

where the $Q(x, y)$ is the integer DN of the registered image, the vector (x, y) is the location in the adjusted coordinate system, P_{ij} represent DNs of the sixteen points surrounding the point (x, y) as shown in Fig. 2, and $\text{sinc}(x) = \sin(\pi x) / (\pi x)$.   The vector (s, t) represents phase of two directions with each element raging from 0 to 1, and this is a random variable of 2-D uniform probability distribution, as we assumed.   Therefore, by assuming there is no quantization in Eq. (3), the DN of the registered image, $Q(x, y)$, is:

$$Q(x, y) \approx \text{int}(gain_b \iint s_b(\alpha, \beta) SPSF(x - \alpha, y - \beta) \, d\alpha d\beta + offset_b) \qquad (5a)$$

$$SPSF(x, y) = \sum_{i=1}^{4} \sum_{j=1}^{4} W_{ij} PSF(x - x_{ij}, y - y_{ij}) \qquad (5b)$$

and $\qquad [W_{ij}] = \begin{bmatrix} \text{sinc}(1+t) \\ \text{sinc}(t) \\ \text{sinc}(1-t) \\ \text{sinc}(2-t) \end{bmatrix} [\text{sinc}(1+s) \quad \text{sinc}(s) \quad \text{sinc}(1-s) \quad \text{sinc}(2-s)] \qquad (5c)$

where the vectors (x_{ij}, y_{ij}) represents the pixel center locations of the surrounding sixteen points. The Eq. (5a), (5b) and (5c) describe the DN of a pixel is a random variable. Thus, the DN of the same target varies from acquisition to acquisition even in normal, non-disaster condition.

Registration errors always remain even if sub-pixel accuracy is achieved in registration, and this increases the randomness of DNs. Obviously, there exist other well-known factors that increase the randomness: electronic noise in sensor system, atmospheric correction error, solar position difference (shade, shadow, etc.), phenological change, soil moisture difference, relative ground sampling interval changing along the off-nadir scan angle, etc. The quantization error in Eq. (3), which we assumed to be negligible in the formulation, is also one of the factors.
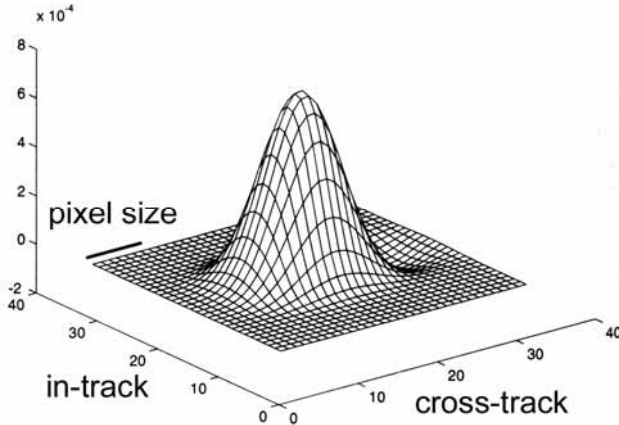

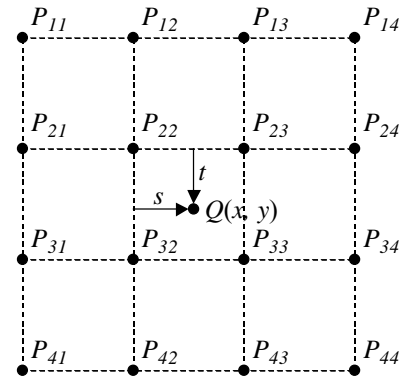**Figure 1.** Point spread function of Landsat/TM (Schowengerdt, 1997).

Figure 2. Registration by cubic convolution.

4 NUMERICAL EXPERIMENT ON DIGITAL NUMBER FLUCTUATION DUE TO DIFFERENCE OF SAMPLE-SCENE PHASE

In this Section, a numerical experiment is conducted to demonstrate that, even if radiometric effects are totally removed, there still exist other causes that generate fluctuations of the DNs of pixels in which there is no physical change over the time; this fluctuation must be considered when damage detection are conducted. In this experiment, a high-resolution image acquired by QuickBird satellite is utilized to simulate middle-resolution images. The synthetic images are generated by considering a flat weighted point spread function for simplicity. Different offset values (sample-scene phases) are used to produce synthetic images taken over the same area at different time to simulate multi-temporal imagery.

4.1 Datasets used in the experiment

To generate synthetic images of middle-resolution, a high-resolution QuickBird image of Boumerdes City, Algeria, is used (Table 1). In the experiment, a sub-scene of approximately 1.5×1.5 km^2, shown in Fig. 3(a), was extracted, which includes urbanized as well as vegetated areas. This area was selected in order to quantify the fluctuation model of the digital numbers in the spatial domain as well as in the spectral domain, i.e. for quantification for different visible and infrared bands.

Table 1. Information on QuickBird high-resolution image used in the experiment.

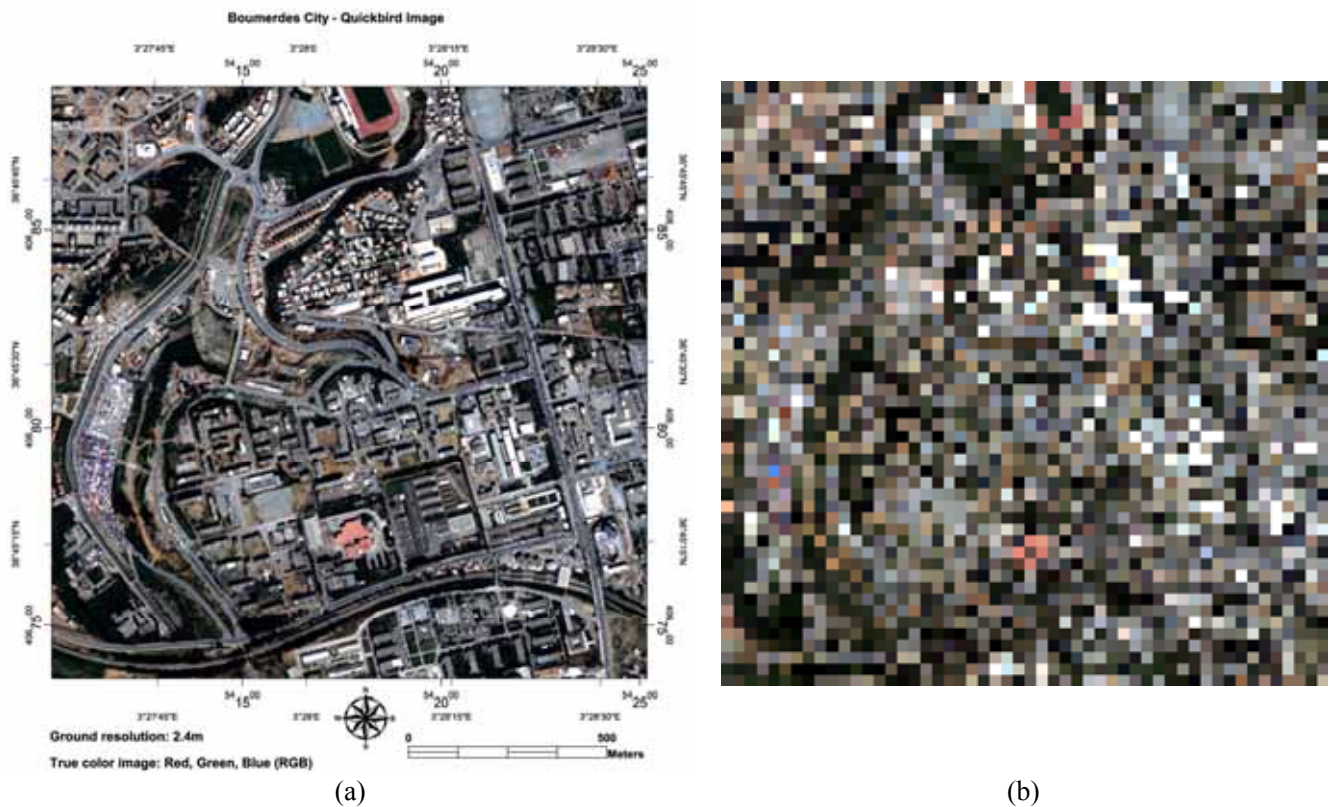| Ground Sampling Distance (m)	Pixels/Lines	Bands	Off nadir angle	Acquisition date and time
2.4	624/624 ($\approx 1.5 \times 1.5$ km^2)	blue, green, red, infrared	$11.2451°$	2002-04-22/10:38:03 (UTC)

Figure 3. Sub-scene of Boumerdes City, Algeria. (a) QuickBird image with ground sampling distance of 2.4 m, true-color, (b) synthetic middle-resolution image, with ground sampling distance of 28.8 m.
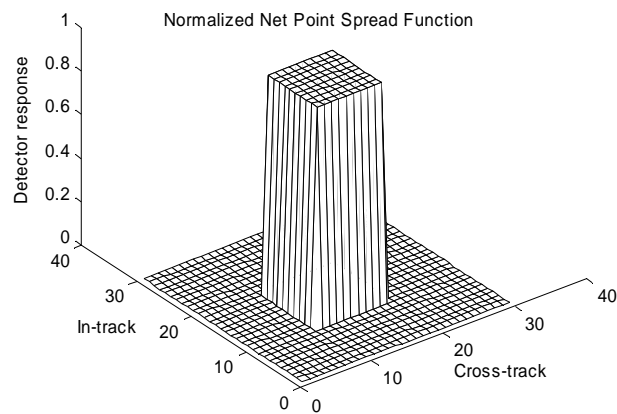

Figure 4. Point spread function used in the numerical experiment.

4.2 Generation of middle-resolution images

The details in an image blur due to the spatial responsivity of the sensor system. The blurring is characterized by the net PSF that is a weighting function for the spatial convolution. In this experiment, a flat weighted PSF (Fig. 4) is used to produce middle-resolution images for simplicity. The pixel DN of the synthetic image is the average of the 12 high-resolution pixels' DN. Since the pixel size of the high-resolution image is 2.4×2.4m, that of the middle-resolution image pixel is 28.8×28.8m, which is as large as the pixel size of Landsat-ETM+

sensor as shown in Fig. 3(b). In order to simulate the DNs of the middle-resolution images, the DNs are quantized into 8-bit integer while DNs of QuickBird images are in 11-bit.

4.3   Simulation of multi-temporal images

The sample-scene phase (offset) changes from acquisition to acquisition process. Since satellites do not pass over the same position even though it flies on the same orbit pass, the offset distances vary among images taken over the same area at different times. This is simulated by moving the averaging window with a certain number of pixels in the high-resolution image. In this experiment, different levels of offsets were studied; the offsets of 0, 1, 3, 6, 9, and 12 pixels in high resolution image was used, which represent 0, 1/12, 1/4, 1/2, 3/4, and 1 pixel in the middle-resolution image.

4.4   Registration of images

Damage detection methods are based on change detection techniques, which require images registered quite accurately to detect change (damage) with high reliability. Hence, the registration must be done to the sub-pixel level. The most common method used for the registration of two or more images is the determination of ground control points (GCP), which tie the reference and the target images. The establishment of GCP may be conducted manually by deploying pairs of points in the reference and template images respectively, or if a geographic map is available, each image can be registered to the map separately. These processes have two disadvantages: firstly, it is time consuming if the images are large, and secondly they are analyst-dependent.

In this experiment an automated method for the selection of GCP is developed. The pixels of the reference and target images of middle-resolution are subdivided up to one twelfth of their size applying cubic convolution interpolation. Once the images are subdivided, 10 sub-scenes of the target image are selected, then, each one is overlaid on the reference image and the cross-correlation is calculated; this process is conducted for every possible location throughout the reference image. The position where the cross-correlation is the maximum is selected as the location of the GCPs. Note that these positions are calculated in steps of one twelfth of the pixel of the middle-resolution image. Once the GCPs are found the target middle-resolution images are registered to the reference image. Since we know how much the misregistration offsets are, the accuracy of registration can be verified.

4.5   Experiment results and discussions

Table 2 shows the errors in the above-mentioned registration process. In the worst case the error is 1.6 pixels; it means 1.6×2.4 m = 3.84 m, about 13% of the pixel size of the middle-resolution image. To achieve an error of only 10% in the detection of change (damage), registration accuracies of 1/5 of pixel size (20%) or less are required (Dai and Khorram, 1998). Hence, the image registration method worked satisfactorily.

Table 2.   Cross-correlation value (C-C) and error (in pixels) in registration of images with the different offsets.

| Offset	2.4m		7.2m		14.4m		21.6m		28.8m	
Template	C-C	Error	C-C	Error	C-C	Error	C-C	Error	C-C	Error
01	0.9971	0	0.9844	1	0.9666	0	0.9827	1	1	0
02	0.9964	0	0.9807	1	0.9560	1	0.9807	1	1	0
03	0.9970	0	0.9829	1	0.9655	0	0.9836	1	1	0
04	0.9958	1	0.9744	2	0.9276	1	0.9665	1	1	0
05	0.9963	0	0.9782	1	0.9597	1	0.9826	1	1	0
06	0.9966	0	0.9799	1	0.9592	1	0.9844	1	1	0
07	0.9971	0	0.9825	1	0.9612	0	0.9831	1	1	0
08	0.9946	1	0.9626	2	0.9173	2	0.9697	2	1	0
09	0.9955	1	0.9656	3	0.8816	5	0.8337	1	0.8242	2
10	0.9936	1	0.9639	3	0.9047	4	0.8878	0	0.9054	1
Average		0.4		1.6		1.5		1		0.3
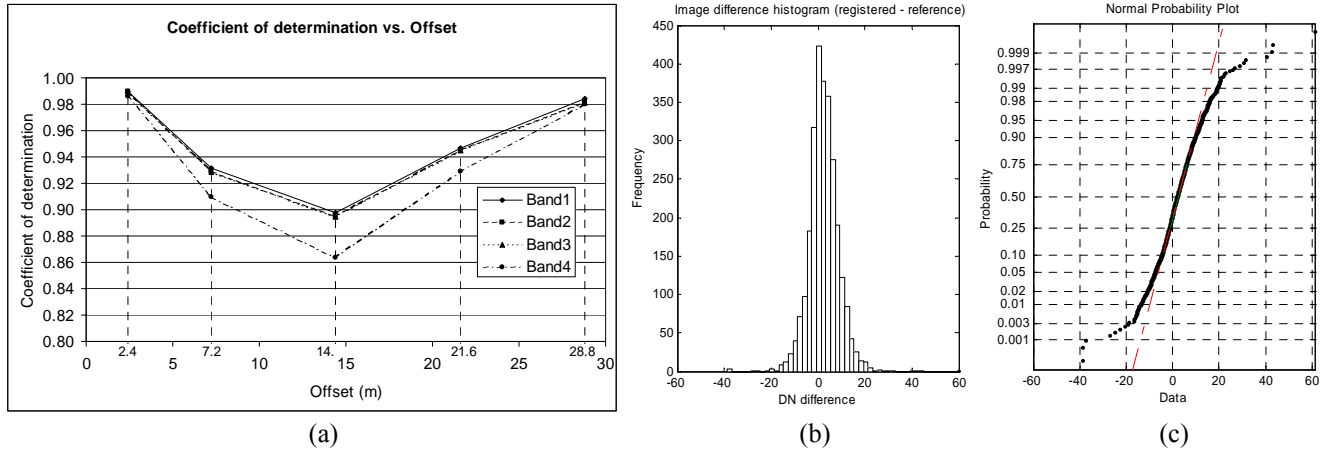
Figure 5. (a) Coefficients of determination (R^2) between the registered and the reference images along with offset distances; (b) histogram and (c) normal probability plot of the digital number difference between the two images with respect to band 4 for an offset of 14.4 m.

After registration of the images, scattergrams of DNs between the registered and the reference images are made, and the coefficients of determination (R^2) are evaluated as a measure of variability, of which higher values denote lower variability. As we can see in Fig. 5(a), the coefficient of determination is high for the images that have small phase difference. Note that the phase decreases when the offset exceeds the half-size of the pixel of the middle-resolution image. Theoretically, the expected value of offset distance that subject to two-dimensional uniform distribution is 0.7652 of the half-size of the middle-resolution pixel.

Even applying the very accurate method of registration (up to 1/12 of pixel size), we can observe that there is still some fluctuation in the values of the digital number that can not be removed; especially this fluctuation is more evident in the infrared band (band 4). Fig. 5(b) shows the histogram of the difference between the corrected and the reference images with the offset of 14.4m. As it can be observed, there still exists variability in the DNs of the pixels that represent the same location on the ground even though there is no change. The normal probability plot is shown in Fig. 5(c) and this suggests that the large amount of DN difference tends to occur more frequently than normal distribution.

5   DAMAGE DETECTION METHOD BASED ON PROBABILITY MODEL OF DIGITAL NUMBERS IN MULTI-TEMPORAL IMAGES

5.1   *Modeling of probability distribution of digital numbers*

As formulated in Section 3, DN of each location can be modeled as a random variable. As the method to evaluate the probability distribution of DN, Eq. (5a), (5b), and (5c) and the two-dimensional uniform distribution of the variables *s* and *t* can be employed. Or, multi-temporal images serve as a sample data to evaluate the probability distribution. Although the number of the pre-event images may be limited, collecting these images is much easier than conventional approaches: gathering reference images of earthquake damage for training data and considering regional differences between the reference and target areas.

The DN fluctuation model for some categorized urban areas is optional solution to increase the sample data, but it may result in decreasing change detection accuracy because pixels with different probability distribution are mixed up and the variance of the categorized model is clearly larger than that of a single pixel model.

5.2   *Damage or change detection based on significance test*

If DN or fluctuation of DN is given as the probability distribution, $Pr(Q)$, range of DN in an image acquired in normal time, i.e. before a disaster. Now, we establish the following null hypothesis:

Null hypothesis H_0:   When the digital number, $q(x, y)$ of the location (x, y) on the ground is acquired, $q(x, y)$ is considered as a sample of the probability distribution, $Pr(Q)$.

and conduct a significance test based on a significance level of α.   If q is in range of small fluctuation and H_0 cannot be rejected, we have no other choice than taking that there is no change on the ground.   But, if rejected, we can judge that there exists an abnormal change on the ground, which exceeds the fluctuation level in normal time, i.e. possibly damage.   Therefore, by conducting the significance test for each location, significance levels , $\alpha(x, y)$,which satisfy the following equation can be evaluated

$$\int_{\mu-|q-\mu|}^{\mu+|q-\mu|} pr(Q)dQ = 1 - \alpha \qquad (6)$$

where $pr(Q)$ is a probability density function of $Pr(Q)$ and μ is the mean of the distribution (Fig. 6).   Note that $Pr(Q)$ can be any probability distribution other than normal distribution, but the mean μ must be given in order to identify the significance level α from Eq. (6).

The DN fluctuation model for some categorized urban areas is optional solution to increase the sample data, but it may result in decreasing change detection accuracy because pixels with different probability distribution are mixed up and the variance of the categorized model is clearly larger than that of a single pixel model. Finally, the map of credibility (probability) of damage occurrence will be obtained by mapping the distribution of the risk percentage (significance level) $1-\alpha$.
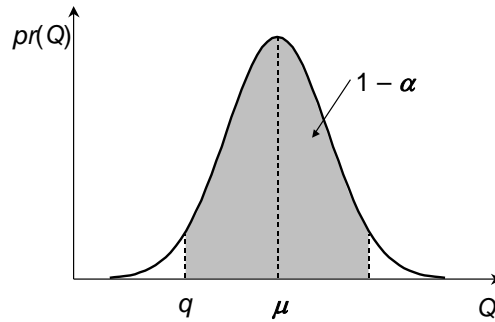

Figure 6.   Evaluation of risk percentage (significance level), $1-\alpha$.   In this example, q, which is a digital number acquired after a disaster, is smaller than μ.

5.3   Damage detection flow

The Fig. 7 shows the flow chart of our proposing method, the Image Fluctuation Model (IFM) method to detect damage (change) using middle-resolution satellite imagery:

Step 1:   Collect the multi-temporal pre-event images
Step 2:   Register these images and compensate atmospheric effects.
Step 3:   Evaluate probability distribution, $Pr(Q)$, for each DN using the above processed images.
Step 4:   Acquire the post-event image.
Step 5:   Process the post-event image for registration and atmospheric correction.
Step 6:   Conduct the significance tests on a pixel basis for all the pixels in a target area using the probability models, $Pr(Q)$, by assuming the null hypothesis that DN is a sample of $Pr(Q)$ with the significance level α.
Step 7:   Create thematic map of $1 - \alpha$ to depict damage (change) probability of each pixel.

Any value of band data, index, or principal component can be the input variable Q; and you can easily expand the dimension of Q and $Pr(Q)$ into higher order by introducing multi-dimensional probability distribution.

If multi-dimensional Gaussian distribution is assumed as a DN fluctuation model, the contour surfaces of α become hyper-ellipsoid (Fig. 8). This seems to be similar to the Ellipsoidal Change Detection (ECD) method proposed by Dai and Khorram (1998), which employs a Gaussian distribution and the Mahalanobis distance function of n-dimensional difference image. But our IFM method substantially differs to ECD; threshold setting is not required anymore while ECD requires that. The result thematic map of IFM method shows the significance level of each pixel area, and it reflects the credibility of the possible damaged area.
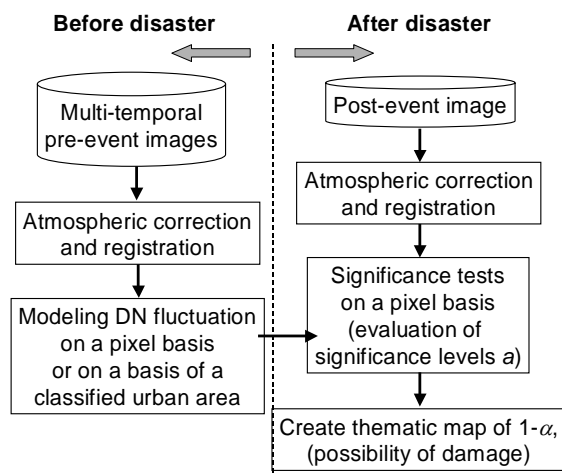

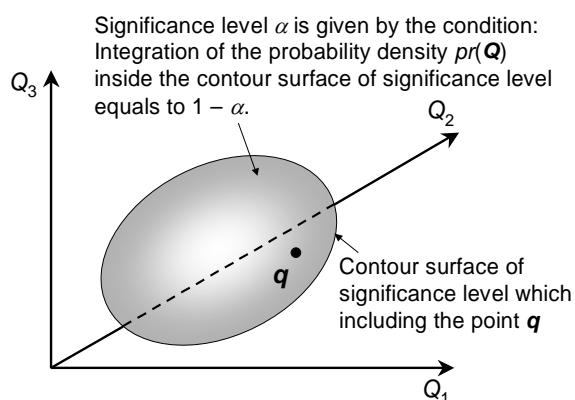**Figure 7.** Flowchart of the Image Fluctuation Model method.

Figure 8. Determination of significance level α when the fluctuation model of digital numbers is expanded to multidimensional probability distribution.

6 CONCLUSIONS

A new damage (change) detection method, the image fluctuation model (IFM) method using middle-resolution satellite images, is proposed, which employs the probability distribution model of the DN fluctuation in a normal condition and its significance test. The result thematic map is created from the significance level to reject the null hypothesis that the pixel DN can be considered as a sample of the DN fluctuation model. The validity of the modeling, and accuracy of the IFM method should be examined based on real satellite images and the application results of actual earthquake cases.

ACKNOWLEDGEMENT

REFERENCES

Dai, X. and Khorram, S. (1998). "The effects of image misregistraion on the accuracy of remotely sensed change detection." *IEEE Transactions on Geoscience and Remote Sensing*. Vol. 36, No. 5, pp.1566-1577.

Kohiyama, M., Hayashi, H., Maki, N., Higashida, M, Kroehl, H.W., Elvidge, C.D., and Hobson V.R. (2003). "Early damaged area estimation system using DMSP/OLS night-time imagery." *International Journal of Remote Sensing* (*in press).*

Morisette, J.T., Khorram, S., and Mace, T. (1999). "Land-cover change detection enhanced with generalized linear models." *International Journal of Remote Sensing*. Vol. 20, No. 14, pp. 2703-2721.

Schowengerdt R.A. (1997). *Remote Sensing: Models and Methods for Image Processing*. Second Edition, Academic Press, San Diego, USA.

Singh, A. (1989). "Digital change detection techniques using remotely-sensed data." *International Journal of Remote Sensing*. Vol. 10, No. 6, pp. 989-1003.